RESEARCH ARTICLE

A Novel Endoscopic Cerenkov Luminescence Imaging System for Intraoperative Surgical Navigation

Tianming Song, Xia Liu, Yawei Qu, Haixiao Liu, Chengpeng Bao, Chengcai Leng, Zhenhua Hu, Kun Wang, and Jie Tian

Abstract

Cerenkov luminescence imaging is an emerging optical technique for imaging the distribution of radiopharmaceuticals in vivo. However, because of the light scattering effect, it cannot obtain optical information from deep internal organs. To overcome this challenge, we established a novel endoscopic Cerenkov luminescence imaging system that used a clinically approved laparoscope and an electron-multiplying charge-coupled device camera. We assessed the performance of the system through a series of in vitro and in vivo experiments. The results demonstrated superior superficial imaging resolution (0.1 mm), a large field of view (500 mm^2 with 10 mm imaging distance), and superb imaging sensitivity (imaging 1 μCi) of our system. It captured the weak Cerenkov signal from internal organs successfully and was applied to intraoperative surgical navigation of tumor resection. It offered objective information of the tumor location and tumor residual during the surgical operation. This technique holds great potential for clinical translation.

CERENKOV RADIATION (CR) was first experimentally detected by Pavel Cerenkov in 1934[1]; then Frank and Tamm proved the physical principle in 1937.[2] Cerenkov luminescence is the electromagnetic radiation emitted when a charged particle passes through a dielectric medium at a speed greater than the phase velocity of light in that medium.[1–4]

In recent years, as the highly sensitive charge-coupled device camera developed rapidly, CR was applied in optical imaging gradually and became an important modality of optical molecular imaging.[5–30] Robertson and colleagues employed CR for in vivo molecular imaging studies for the first time, and novel Cerenkov luminescence imaging (CLI) was presented.[5] Considering the positron energy spectrum, Spinelli and colleagues presented a detailed model of the CR spectrum to quantify the CR emission.[6] Although CLI has demonstrated many advantages, such as high superficial resolution, high throughput, low cost, ability to use clinically approved radioactive tracers,[12–25] and great potential of clinical translation,[17,18] conventional planar CLI still cannot reflect depth information under skin tissues. Therefore, considerable efforts were made in three-dimensional Cerenkov luminescence tomography techniques, and a variety of approaches have been proposed with certain promise.[7–12] However, these methods did not solve the essential challenge of acquiring optical information from deep organs, only offering limited imaging depth because a great portion of Cerenkov light was lost due to the tissue absorption and scattering effect.

Endoscopic imaging provides another option by maximally reducing the optical signal loss through minimum invasion, which can effectively avoid tissue absorption and scattering.[26–30] Here we present a novel endoscopic Cerenkov luminescence imaging (ECLI) system that used a clinically available endoscope to achieve high-resolution and high-sensitivity in vivo imaging of radioactive tracer with a large field of view (FOV). The system was validated by a series of in vitro and in vivo studies and then applied to in vivo tumor detection and intraoperative surgical navigation. The ECLI system holds great promise for clinical translation of tumor detection in deep internal organs.

Materials and Methods

ECLI System

The ECLI system consisted of three units, as shown in Figure 1. The electronic x-y-z translation platform and the animal cage constituted the animal holding unit (see Figure 1A). The

From the School of Automation, Harbin University of Science and Technology, Harbin, China; Key Laboratory of Molecular Imaging, Chinese Academy of Sciences, Beijing, China; and Department of Gastroenterology, General Hospital of Chinese People's Armed Police Forces, Beijing, China.

Address reprint requests to: Xia Liu, School of Automation, Harbin University of Science and Technology, 95 XueFu Road, 150080, Harbin, China; e-mail: liuxia@hrbust.edu.cn; Zhenhua Hu, Kun Wang or Jie Tian, Key Laboratory of Molecular Imaging, Institute of Automation, Chinese Academy of Sciences, 95 ZhongGuanCun East Road, 100190, Beijing, China; e-mails: zhenhua.hu@ia.ac.cn; kun.wang@ia.ac.cn; jie.tian@ia.ac.cn.

DOI 10.2310/7290.2015.00018

DECKER

Cerenkov signal acquisition unit (see Figure 1B) employed a clinically available laparoscope (WA53000A, Olympus, Japan; length 400 mm, diameter 10 mm) coupled with an electron-multiplying charge-coupled device (EMCCD) camera (DU888+, Andor Technology, Belfast, UK). The sensor size of the EMCCD camera is 13.3 × 13.3 mm with a total pixel number of 1,024 × 1,024. The laparoscope and EMCCD camera were connected by a custom-made adapter so that the focus could be adjusted manually by turning the spin button on it. The control and display unit consisted of a computer and a controller of the animal holding unit (see Figure 1C). It also controlled the parameters of the acquisition unit, such as exposure time, binning, and gain. The animal holding unit and Cerenkov signal acquisition unit were installed in a light sealing box inside a dark room to prevent interference from the background light noise.

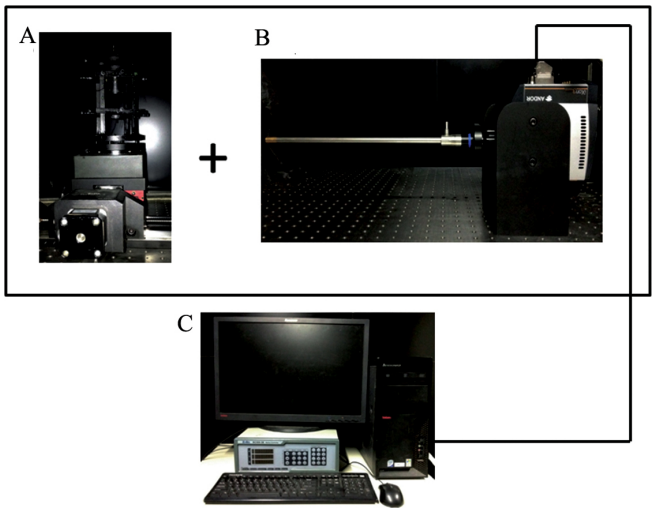

Figure 1. The endoscopic Cerenkov luminescence imaging system. *A*, Animal holding unit: an animal cage was put on top of an electronic x-y-z translation platform. *B*, Cerenkov signal acquisition unit: a laparoscope was coupled with an EMCCD camera by a custom-made adapter. Both *A* and *B* were installed in a light sealing box. *C*, A control and display unit controlled the translation platform and the imaging acquisition parameters.

To investigate the performance of the ECLI system, a series of in vitro and in vivo studies were conducted.

CLI System

The conventional planar Cerenkov luminescent images were acquired by a CLI system developed in our laboratory. The system consisted of a lens (24 mm, F1.4, Canon, Japan) coupled with the same DU888+ camera (Andor Technology, Belfast, UK) as the ECLI system. The planar Cerenkov luminescent images were obtained under the same environment and the same light sealing.

In Vitro Phantom Studies

A multifunctional calibration target (NT58-403, Edmund Optics, Barrington, NJ; Figure 2A was imaged by the ECLI system in room light to evaluate the FOV in the function of

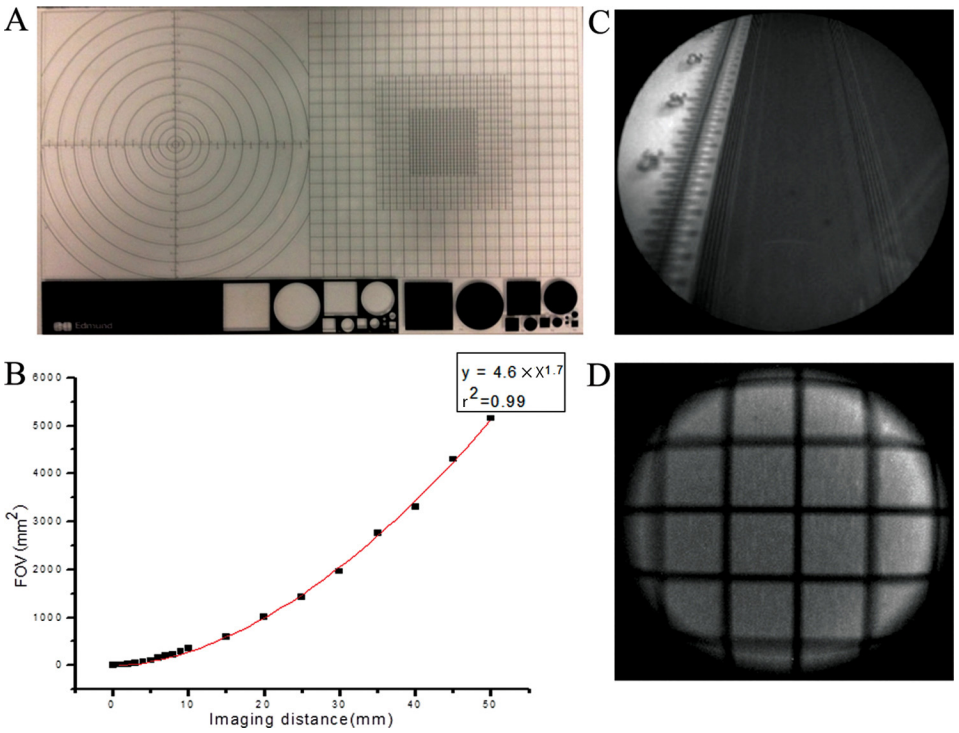

Figure 2. Endoscopic Cerenkov luminescence imaging (ECLI) system performance assessment. *A*, The field of view (FOV) increased exponentially in the function of imaging distance. *B*, A multifunctional calibration target. *C*, Standard phantom showed that the imaging resolution of the ECLI system was 0.1 mm. *D*, The fish-eye effect of the ECLI system.

the imaging distance, the imaging resolution, and the geometric distortion. Then [^{18}F]fluorodeoxyglucose ([^{18}F]FDG) (0.3 mL, 160 μCi, concentration 0.53 μCi/μL) was injected into an Eppendorf (EP) tube, and a series of luminescent images were acquired using the ECLI system at different time points so that the system's sensitivity was evaluated via different radioactivities (160 μCi, 80 μCi, 40 μCi, 20 μCi, and 1 μCi) of the same imaging subject in the sealed light environment. The imaging parameters were exposure 300 seconds, gain 800, and no binning for all cases except for imaging the 1 μCi tube, in which binning 4 was applied. Although the EMCCD camera was placed away from the imaging subjects due to the length of the laparoscope (see Figure 1B), a small portion of the high-energy gamma photons (511 keV) emitted from [^{18}F]FDG still reached the chip of the EMCCD camera and caused background noise (Figure S1, left image, online version only). Therefore, imaging filtering was applied to eliminate the noise effect (Figure S1, right image, online version only). This technique was applied to all image acquisitions in this study.

To investigate the performance of the ECLI system for imaging radioactive tracers with various depths, we prepared three glass tubes (diameter 2 mm, length 22 mm) filled with 150 μCi [^{18}F]FDG (concentration 2.17 μCi/μL). The tubes were arranged in a row 10 mm apart. Then five pieces of porcine muscle tissue with different thicknesses (1–5 mm) were placed on the tubes, and the luminescent images were acquired separately by the ECLI system.

Animal Experiments

All animal experiments were performed in accordance with the guidelines of the Institutional Animal Care and Use Committee (IACUC) at Peking University (Permit Number 2011-0039), which also approved the research procedures. All surgery was performed under sodium pentobarbital anesthesia, and all efforts were made to minimize suffering. All the nude mice were female, 5 to 6 weeks old, and purchased from the Department of Experimental Animals, Peking University Health Science Center. Human colon carcinoma cells HCT-8 were cultured in Dulbecco's Modified Eagle's Medium (DMEM). Cells were grown in a humidified air atmosphere of 5% CO_2 at a temperature of 37°C. Approximately 1×10^6 HTC-8 cells were implanted subcutaneously in the left underarm of each nude mouse.

In Vivo Studies

[^{18}F]FDG (500 μCi, concentration 3.7 μCi/μL) was injected into three healthy nude mice via the tail vein. Conventional Cerenkov luminescence images were acquired 30 minutes after the injection using the CLI system. Then for each mouse, the chest and abdomen area was surgically opened, and the ECLI system was applied to acquire the luminescent images of internal organs (exposure 300 seconds, gain 800, and binning 4). After that, the mice were sacrificed immediately, and the radioactivity of the internal organs within the FOV was measured to compare the optical intensity measured from images.

After imaging the healthy nude mice, a HCT-8 tumor xenograft mouse model was employed for simulating the intraoperative tumor resection using the ECLI system. [^{18}F]FDG (640 μCi, concentration 4.27 μCi/μL) was injected into the xenograft tumor model via the tail vein, and luminescent images with different FOV were acquired (exposure 300 seconds, gain 800, and binning 4) before and after surgery. Surgical resection was operated by an experienced surgeon. Hematoxylin-eosin microscopy was applied to verify the resected tissue.

Results

ECLI System In Vitro Evaluation

In the optical property evaluation of the system, we found that the FOV increased exponentially with an increase in imaging distance, as shown in Figure 2B ($Y = 4.6 \times X^{1.7}$, $r^2 = .99$). When the tip of the laparoscope was 10 mm away from the imaging subject, the FOV reached 500 mm^2. The maximal superficial resolution of the system was 0.1 mm (see Figure 2C). The barrel distortion became more and more severe from the center of FOV to the surrounding periphery (see Figure 2D). This was probably because the laparoscope is a 0° angle endoscope with a typical fish-eye lens effect.

In the Cerenkov signal sensitivity evaluation, we found that the Cerenkov luminescent signal emitting from 1 μCi [^{18}F]FDG was detected using the ECLI system (Figure 3A, bottom right image), and 1 μCi was the minimal detectable dose. To receive such a weak optical signal, the imaging distance had to be less than 10 mm. That was why the FOV was smaller for imaging 20 μCi and 1 μCi [^{18}F]FDG (see Figure 3A). The quantitative analysis showed that the Cerenkov light signal increased linearly in the function of the radioactivity (Figure 3B), which was consistent with the findings of other optical imaging systems.[13,14,23] The correlation coefficient was $r^2 = .97$.

In the imaging depth evaluation, the ECLI system detected Cerenkov luminescent signal of 150 μCi [^{18}F]FDG under 5 mm thick porcine muscle tissue (Figure 4A, right image). However, the structural information of the light sources was almost lost in the last two cases (4 mm and 5 mm depth) because of the scattering effect. The plots in Figure 4B are the line profiles across the three glass tubes (red lines on

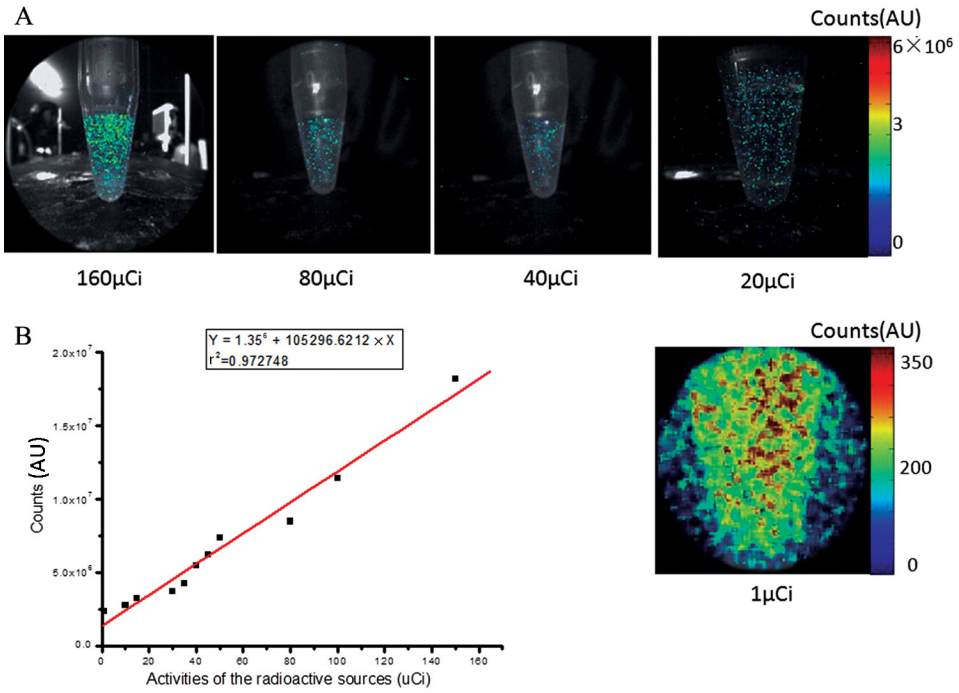

Figure 3. In vitro sensitivity assessment of the endoscopic Cerenkov luminescence imaging system. *A*, The luminescence images of 160 μCi, 80 μCi, 40 μCi, 20 μCi, and 1 μCi [^{18}F]FDG, respectively. *B*, The linear relationship between Cerenkov signal and the activities of [^{18}F]FDG. AU = arbitrary units

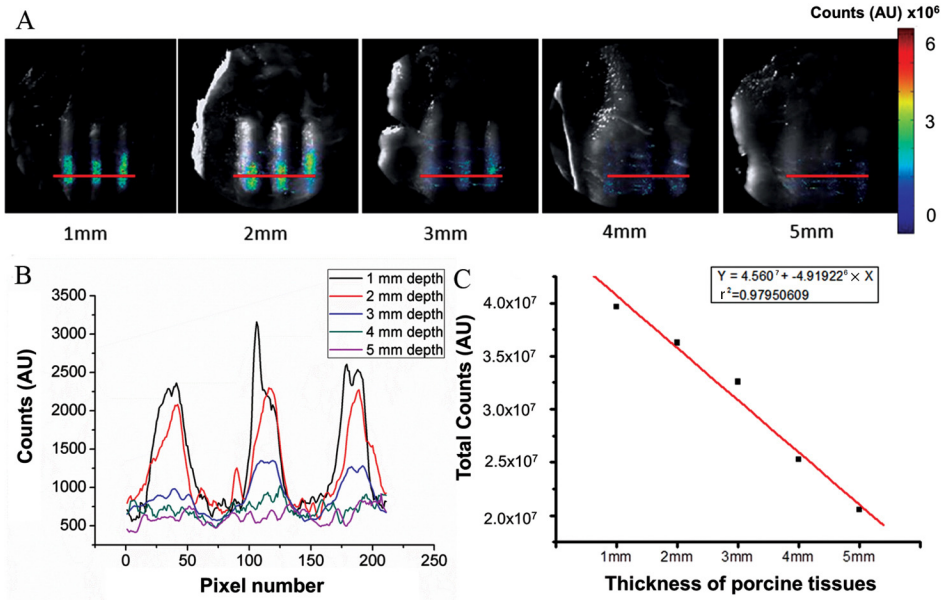

Figure 4. In vitro imaging depth assessment of the endoscopic Cerenkov luminescence imaging (ECLI) system. *A*, Porcine muscle tissues with different thicknesses were put on top of three glass tubes filled with 150 μCi [^{18}F]FDG. The overlay of white light and luminescent images was acquired by the ECLI system. *B*, The line profiles across the three glass tubes in different imaging depths. The *red lines* in *A* indicate the location of the profiles. *C*, The linear relationship between the signal intensity and thickness of porcine muscle tissues. AU = arbitrary units

Figure 4A) in different imaging depths, which revealed that the ECLI system can sufficiently distinguish the morphology of the imaging subjects up to 3 mm imaging depth. We also found the linear relationship between the Cerenkov signal and the imaging depth (r^2 = .98; Figure 4C).

ECLI for In Vivo Applications

Three healthy nude mice were injected via the tail vein with 500 μCi [^{18}F]FDG (concentration 3.7 μCi/μL). Figure 5 illustrates the comparison of the images acquired from the

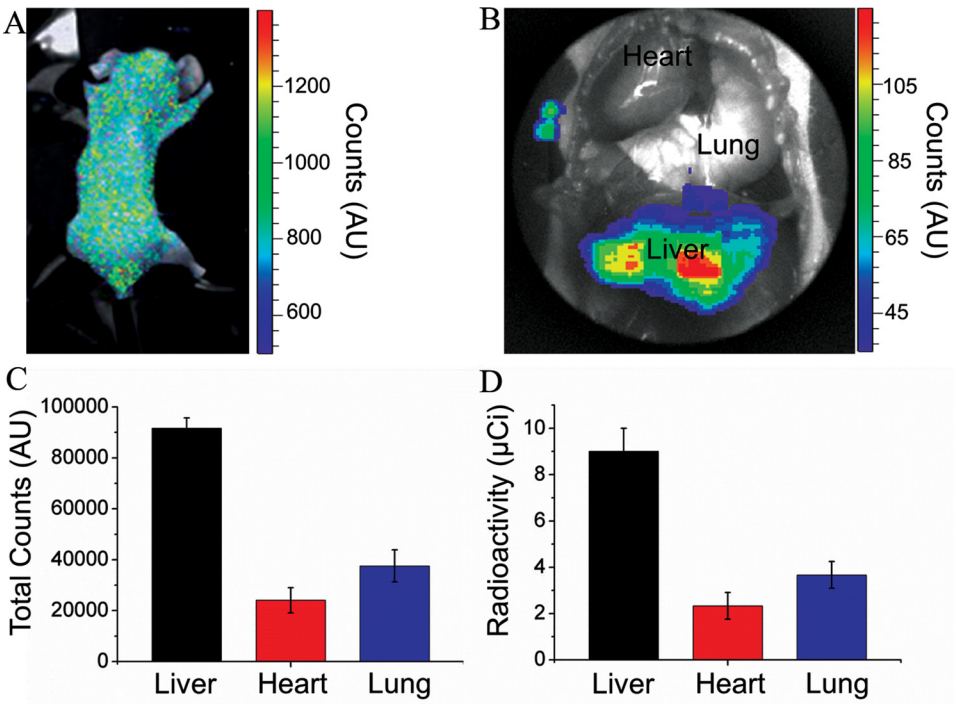

Figure 5. In vivo comparison of images acquired from Cerenkov luminescence imaging (CLI) and endoscopic Cerenkov luminescence imaging (ECLI) systems. *A* and *B* are the overlay images acquired from the CLI and ECLI systems. *C*, The average optical signal intensity of the liver, heart, and lung quantified from the ECLI imaging of the three mice. *D*, The average radioactivity of the liver, heart, and lung. AU = arbitrary units

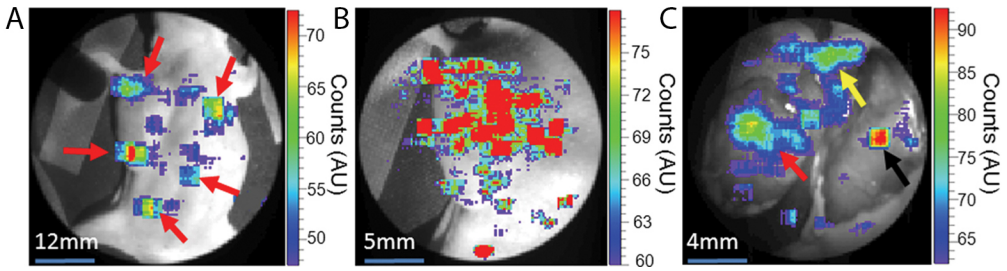

Figure 6. Similation of intraoperative surgical navigation using the endoscopic Cerenkov luminescence imaging (ECLI) system. *A*, Due to the large imaging distance and noise, a whole body overlay image showed several suspicious areas (*red arrows*). *B*, With a much smaller imaging distance, the ECLI system captured significant optical signal from the tumor tissue. *C*, After surgical resection of the tumor tissue (*red arrow*), tumor residuals (*yellow and black arrows*) were detected by the ECLI system. AU = arbitrary units

CLI and ECLI systems. The Cerenkov luminescent flux was clearly captured on the surface of the mouse using the CLI system (see Figure 5A). However, it was difficult to estimate the [^{18}F]FDG metabolism of the major internal organs due to the severe light scattering. For the same imaging subject, the ECLI system was able to acquire images through minimum invasion (see Figure 5B). The image clearly revealed that 50 minutes after the tail vein injection, most of the Cerenkov luminescence came from the liver, and [^{18}F]FDG was not homogeneously distributed in the liver. After sacrificing the mice, the average radioactivity of the liver, heart, and lung was 9.0 ± 1.0 μCi, 2.3 ± 0.6 μCi, and 3.7 ± 0.6 μCi, respectively (Figure 5D). The optical signal intensity of the three organs was (9.2 ± 0.4) × 10^4, (2.4 ± 0.5) × 10^4, and (3.8 ± 0.6) × 10^4, respectively (Figure 5C). The optical signal intensity obtained from the ECLI system matched the radioactivity of the mice internal organs.

[^{18}F]FDG (640 μCi, concentration 4.27 μCi/μL) was injected into an HCT-8 xenograft tumor model via the tail vein, and the ECLI system was employed for intraoperative tumor detection. The tumor tissue was resected by a surgeon based on his experience, and several Cerenkov luminescent images were acquired before and after resection using our ECLI system (Figure 6).

Before the surgery, a whole body luminescent image was taken (see Figure 6A) to locate the tumor (FOV 2,700 mm^2). However, because the imaging distance was too large and the aperture of the laparoscope was relatively small, several regions of interests (ROI) with high signal intensity can be seen (see Figure 6A, red arrows). By using the electronic x-y-z translation platform, we decreased the imaging distance, which resulted in a smaller FOV. But after scanning all of these suspected ROI, only the tumor tissue showed significant optical signals (see Figure 6B; FOV 500 mm^2). The other ROI were just random noise. Then the surgeon performed the operation and left the resected tissue next to the wound. Another luminescent image was acquired by the ECLI system to verify the residual tumor tissue (see Figure 6C; FOV 400 mm^2). We found clear optical signal from the resected tissue (see Figure 6C, red arrow), the center of the wound (see Figure 6C, black arrow), and the skin of the upper area of the wound (see Figure 6C, yellow arrow). This indicated that significant tumor residual was not removed during the surgery, and further resection needed to be proceeded. We also measured the radioactivity of the resected tumor tissue, which was 5 μCi. After resecting the residual tissue, hematoxylin-eosin microscopy confirmed that the tumor tissue was positive (Figure S2, online version only).

Discussion

This study demonstrated a novel ECLI system to detect Cerenkov luminescent signals in vivo effectively. The system used a clinically available laparoscope to acquire white light and luminescent images with minimum invasion. Since the radioactive tracer and the laparoscope are both approved by the US Food and Drug Administration, this system showed great potential for clinical translation.

We evaluated the performance of the ECLI system through a series of in vitro and in vivo experiments. It can provide great imaging resolution (superficial), large FOV, and superb optical sensitivity. The inherent advantages of the endoscopic imaging help this system overcome the challenge of detecting weak Cerenkov signals from deep internal organs in vivo. We found consistent correlation between Cerenkov signal intensity and radioactivity of different internal organs.

We employed the ECLI system to perform an intraoperative surgical navigation for resection of the tumor tissue of a HCT-8 xenograft. The results were encouraging. With the help of the ECLI system, we were able to locate the tumor tissue preoperation and examine the tumor residual postoperation. This technique will significantly impact the detection and resection of tumor lesions inside the peritoneal cavity.

The biggest challenge regarding the idea of using endoscopic systems for Cerenkov imaging is always the sensitivity.[18–20,28–30] Compared to conventional CLI systems, the ECLI system can bring the lens extremely close to the ROI (less than 10 mm imaging distance) and still offer large FOV. This advantage compensates the sacrifice of the optical aperture and ensures imaging sensitivity. For our in vivo applications, the minimum dose that could generate effective optical signal from organs or tissues was 5 μCi. However, the tumor lesion uptake of radiopharmaceuticals in clinical human applications was much less than this value, which means that further improvement of the sensitivity is still necessary.

In conclusion, we established a novel ECLI system that can provide excellent superficial imaging resolution, great FOV, and superb imaging sensitivity. This system can overcome the limitation of imaging depth of conventional CLI and offer objective information of tumor location and tumor residual during tumor resection surgery. This technique holds great potential for clinical translation.

Acknowledgments

Financial disclosure of authors: This work was supported by the National Basic Research Program of China (973 Program) under Grant No. 2011CB707700; the National Natural Science Foundation of China under Grant Nos. 81227901, 61172167, 61401462, 61302024, and 81471700; and the Natural Science Foundation of Heilongjiang Province of China under Grant No. F201311. The funders had no role in study design, data collection and analysis, decision to publish, or preparation of the manuscript.

Financial disclosure of reviewers: None reported.

References

1. Cherenkov PA. Visible emission of clean liquids by action of γ radiation. Dokl Akad Nauk SSSR 1934;2:451.
2. Frank IM, Tamm IE. Coherent visible radiation of fast electrons passing through matter. Dokl Akad Nauk SSSR 1937;14:109–14.
3. Čerenkov PA. Visible radiation produced by electrons moving in a medium with velocities exceeding that of light. Phys Rev 1937;52:378, doi:10.1103/PhysRev.52.378.
4. Jelley JV. Cerenkov radiation and its applications. Br J Appl Phys 1955;6:227, doi:10.1088/0508-3443/6/7/301.
5. Robertson R, Germanos MS, Li C, et al. Optical imaging of Cerenkov light generation from positron-emitting radiotracers. Phys Med Biol 2009;54:N355, doi:10.1088/0031-9155/54/16/n01.
6. Spinelli AE, D'Ambrosio D, Calderan L, et al. Cerenkov radiation allows in vivo optical imaging of positron emitting radiotracers. Phys Med Biol 2010;55:483, doi:10.1088/0031-9155/55/2/010.
7. Li C, Mitchell GS, Cherry SR. Cerenkov luminescence tomography for small-animal imaging. Opt Lett 2010;35:1109–11, doi:10.1364/OL.35.001109.

8. Hu Z, Liang J, Yang W, et al. Experimental Cerenkov luminescence tomography of the mouse model with SPECT imaging validation. Opt Express 2010;18:24441–50, doi:10.1364/OE.18.024441.
9. Zhong J, Qin C, Yang X, et al. Cerenkov luminescence tomography for in vivo radiopharmaceutical imaging. J Biomed Imaging 2011; 2011:2, doi: 10.1155/2011/641618.
10. Spinelli AE, Kuo C, Rice BW, et al. Multispectral Cerenkov luminescence tomography for small animal optical imaging. Opt Express 2011;19:12605–18, doi:10.1364/OE.19.012605.
11. Lewis MA, Kodibagkar VD, Öz OK, et al. On the potential for molecular imaging with Cerenkov luminescence. Opt Lett 2010; 35:3889–91, doi:10.1364/OL.35.003889.
12. Mitchell GS, Gill RK, Boucher DL, et al. In vivo Cerenkov luminescence imaging: a new tool for molecular imaging. Philos Trans R Soc A Math Phys Eng Sci 2011;369:4605–19, doi:10.1098/rsta.2011.0271.
13. Xu Y, Liu H, Cheng Z. Harnessing the power of radionuclides for optical imaging: Cerenkov luminescence imaging. J Nucl Med 2011;52:2009–18, doi:10.2967/jnumed.111.092965.
14. Chin PTK, Welling MM, Meskers SCJ, et al. Optical imaging as an expansion of nuclear medicine: Cerenkov-based luminescence vs fluorescence-based luminescence. Eur J Nucl Med Mol Imaging 2013;40:1283–91, doi:10.1007/s00259-013-2408-9.
15. Thorek DLJ, Robertson R, Bacchus WA, et al. Cerenkov imaging—a new modality for molecular imaging. Am J Nucl Med Mol Imaging 2012;2:163.
16. Xu Y, Liu H, Chang E, et al. Cerenkov luminescence imaging (CLI) for cancer therapy monitoring. J Vis Exp 2011;69:e4341–41.
17. Hu Z, Ma X, Qu X, et al. Three-dimensional noninvasive monitoring iodine-131 uptake in the thyroid using a modified Cerenkov luminescence tomography approach. PloS One 2012;7:e37623, doi:10.1371/journal.pone.0037623.
18. Liu H, Carpenter CM, Jiang H, et al. Intraoperative imaging of tumors using Cerenkov luminescence endoscopy: a feasibility experimental study. J Nucl Med 2012;53:1579–84, doi:10.2967/jnumed.111.098541.
19. Kothapalli SR, Liu H, Liao JC, et al. Endoscopic imaging of Cerenkov luminescence. Biomed Opt Express 2012;3:1215–25, doi:10.1364/BOE.3.001215.
20. Thorek DLJ, Riedl CC, Grimm J. Clinical Cerenkov luminescence imaging of 18F-FDG. J Nucl Med 2014;55:95–8, doi:10.2967/jnumed.113.127266.
21. Spinelli AE, Ferdeghini M, Cavedon C, et al. First human Cerenkography. J Biomed Opt 2013;18:020502, doi:10.1117/1.JBO.18.2.020502.
22. Ma X, Wang J, Cheng Z. Cerenkov radiation: a multi-functional approach for biological sciences. Front Phys 2014;2:4, doi:10.3389/fphy.2014.00004.
23. Hu Z, Yang W, Ma X, et al. Cerenkov luminescence tomography of aminopeptidase N (APN/CD13) expression in mice bearing HT1080 tumors. Mol Imaging 2013;12:173–81.
24. Ma X, Wang J, Cheng Z. Cerenkov radiation: a multi-functional approach for biological sciences. Biomed Phys 2014;2:4, doi:10.3389/fphy.2014.00004.
25. Ruggiero A, Holland JP, Lewis JS, et al. Cerenkov luminescence imaging of medical isotopes. J Nucl Med 2010;51:1123–30, doi:10.2967/jnumed.110.076521.
26. Xu Y, Chang E, Liu H, et al. Proof-of-concept study of monitoring cancer drug therapy with Cerenkov luminescence imaging. J Nucl Med 2012;53:312–7, doi:10.2967/jnumed.111.094623.
27. Ding X, Wang K, Jie B, et al. Probability method for Cerenkov luminescence tomography based on conformance error minimization. Biomed Opt Express 2014;5:2091–112, doi:10.1364/BOE.5.002091.
28. Hu H, Cao X, Kang F, et al. Feasibility study of novel endoscopic Cerenkov luminescence imaging system in detecting and quantifying gastrointestinal disease: first human results. Eur Radiol 2015;25:1814–22, doi:10.1007/s00330-014-3574-2.
29. Cao X, Chen X, Kang F, et al. Performance evaluation of endoscopic Cerenkov luminescence imaging system: in vitro and pseudotumor studies. Biomed Opt Express 2014;5:3660–70, doi:10.1364/BOE.5.003660.
30. Carpenter CM, Ma X, Liu H, et al. Cerenkov luminescence endoscopy: improved molecular sensitivity with β-emitting radiotracers. J Nucl Med 2014;55:1905–9, doi:10.2967/jnumed.114.139105.

A Novel Endoscopic Cerenkov Luminescence Imaging System for Intraoperative Surgical Navigation

Tianming Song, Xia Liu, Yawei Qu, Haixiao Liu, Chengpeng Bao, Chengcai Leng, Zhenhua Hu, Kun Wang, and Jie Tian

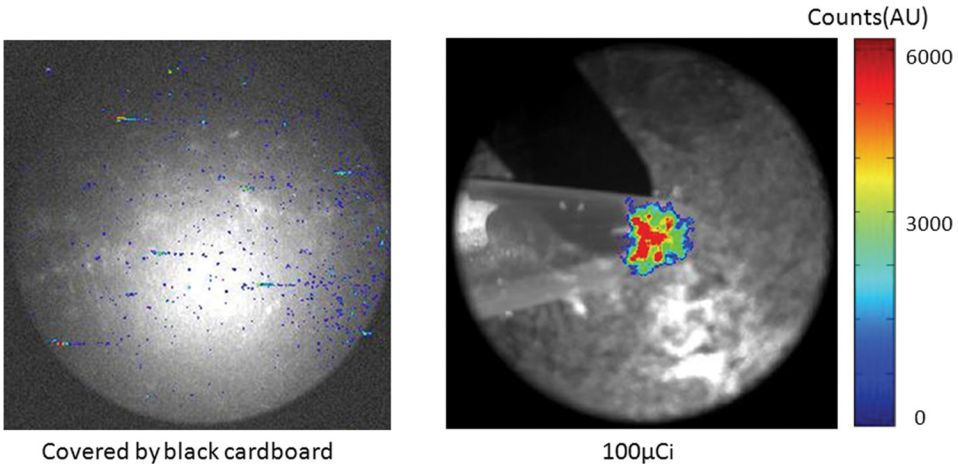

Figure S1. Process of eliminating the noise caused by gamma photons. An EP tube with [^{18}F]FDG (100 μCi, concentration 2 μCi/μL) was covered by black cardboard to exclude the Cerenkov photons. The *left image* shows the row data acquired by the endoscopic Cerenkov luminescence imaging system. It demonstrates the noise effect caused by gamma rays. After applying a simple imaging filtering algorithm, the noise was removed. Thus, the *right image* shows only the Cerenkov luminescent signals. AU = arbitrary units

From the School of Automation, Harbin University of Science and Technology, Harbin, China; Key Laboratory of Molecular Imaging, Chinese Academy of Sciences, Beijing, China; and Department of Gastroenterology, General Hospital of Chinese People's Armed Police Forces, Beijing, China.

Address reprint requests to: Xia Liu, School of Automation, Harbin University of Science and Technology, 95 XueFu Road, 150080, Harbin, China; e-mail: liuxia@hrbust.edu.cn; Zhenhua Hu, Kun Wang or Jie Tian, Key Laboratory of Molecular Imaging, Institute of Automation, Chinese Academy of Sciences, 95 ZhongGuanCun East Road, 100190, Beijing, China; e-mails: zhenhua.hu@ia.ac.cn; kun.wang@ia.ac.cn; jie.tian@ia.ac.cn.

DOI 10.2310/7290.2015.00018

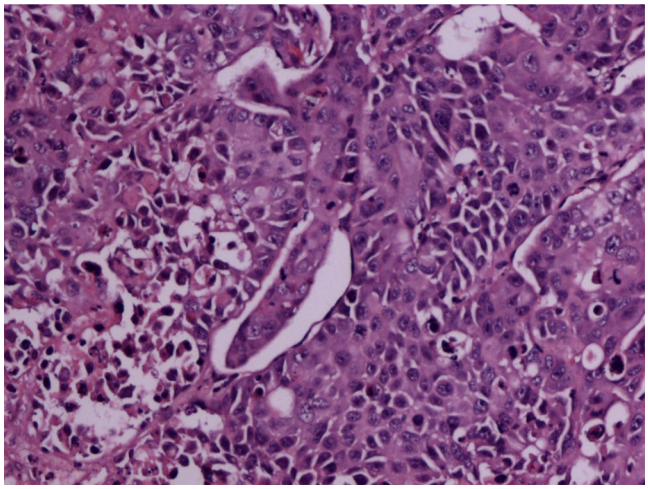

Figure S2. Hematoxylin-eosin histology of the resected residual tissue confirmed that the tumor was positive. Magnification level = ×200.